

# Modeling Soil Reaction to Laterally Loaded Piles

TAKAAKI KAGAWA

A numerical study was made for linearly elastic soil-pile conditions to clarify the lateral soil-reaction behavior of a pile. The apparent lateral stiffness of soil is strongly influenced not only by the soil stiffness but also the geometry and the stiffness of a pile. Also, the apparent lateral stiffness of soil varies significantly with depth, even if the soil stiffness is constant with depth. A new and improved procedure for estimating the lateral soil springs that can be used with the beam-on-Winkler foundation model of a soil-pile system is presented. With these soil springs the beam-on-Winkler foundation model can reproduce with excellent accuracy the pile responses computed from the corresponding continuum system. Although limited to linearly elastic soil-pile conditions, the results may be expanded to nonlinear soil conditions.

Piles have been used extensively to improve the foundation performance of a wide range of transportation systems. In addition, piles are becoming increasingly popular, since new construction and developments must cope with undesirable subsurface conditions involving weak and compressible soils that have been avoided in the past.

It is evident that pile foundations have a controlling impact on the overall performance of a transportation system. However, the most common design practice has been to represent a pile foundation by a set of simplistic linearly elastic translational and rotational springs, lumped at the pile-cap level. These discrete foundation springs are supposed to represent the embedded portion of the pile and the surrounding soil. Their numerical values should reflect the influence of various key soil-pile factors. Such factors include variations of soil properties with depth, geometrical and stiffness properties of the pile, and the constraining condition at the pile cap, among other factors. Therefore, evaluation of such foundation springs is not straightforward. It requires consideration of soil-pile interaction, which is affected by the stiffness and the geometrical properties of soil and pile. Such foundation springs are often determined from available elasticity solutions that assume homogeneity of soil properties with depth. For critical transportation systems, however, such foundation springs should be determined by performing soil-pile interaction analyses that explicitly account for the soil-pile conditions at the project site. The key conditions are the stress-strain-strength behavior of soils at the site and variations of soil-pile stiffness with depth.

In the last 10 years a number of studies have developed various types of numerical methods for soil-pile interaction analyses of single piles and groups of piles. These methods include the finite-element method, the boundary-element

method, mathematical solutions to wave equations, and the beam-on-Winkler foundation method. The finite-element and boundary-element methods are generally costly and may not be readily available to practicing design engineers. Mathematical solutions are limited to idealized soil-pile conditions. Therefore, the most economical and versatile numerical method for soil-pile interaction analyses tends to be the beam-on-Winkler foundation method.

The beam-on-Winkler foundation method approximates the lateral soil reaction, which is continuous with depth, using a series of isolated lateral soil springs. Therefore, the method neglects the interaction between such soil springs. Because of this simplification the method is numerically efficient. The method has also been shown to yield satisfactory pile responses when it is used with appropriate soil springs. Therefore, the reliability of the method is determined by our ability to predict realistic lateral soil springs to be used with the method.

Evaluation of the lateral soil springs for the beam-on-Winkler foundation model is not an easy task. The lateral soil springs are influenced not only by the stiffness properties of soil but also by the geometry and the stiffness properties of a pile. Rational guidelines are not available to estimate the lateral soil springs, even for linearly elastic soil conditions.

The lateral soil springs for the beam-on-Winkler foundation model were first determined by using the concept of subgrade-reaction moduli. The subgrade-reaction moduli were estimated from field plate-loading tests on clays and sands (1-3) and later from field and laboratory pile-load tests. The lateral soil springs thus determined are still being used in pile design.

The lateral soil springs vary dramatically when the magnitude of pile deflection changes. This change is due mainly to the nonlinear stress-strain effects in soil. Therefore, the lateral soil springs based on the subgrade-reaction theory are associated with the magnitude of pile deflections in a test. Considering the nonlinear nature of the lateral soil reaction, McClelland and Focht (4) proposed to relate the lateral load-deflection ( $p$ - $y$ ) relations of pile to the stress-strain relations of soil. This method has been revised by various researchers by using field and laboratory pile-load test results (5-8), and the method is well accepted in offshore pile design (9).

These  $p$ - $y$  criteria, however, are based on pile-load tests with a narrow range of soil-pile parameters. In addition, it is always difficult to quantify the stress-strain relations of soil adjacent to a pile in field tests. Therefore, these  $p$ - $y$  criteria are not necessarily suited to rigorous derivation of the relation between the lateral soil springs ( $p$ - $y$  stiffness) and in situ soil stiffness.

Department of Civil Engineering, 2150 Engineering Building, Wayne State University, Detroit, Mich. 48202.

Kagawa and Kraft (10) studied analytically the lateral soil springs of a linearly elastic soil-pile system. The objectives of this study were to (a) clarify for idealized soil-pile conditions the relation between the  $p$ - $y$  stiffness and the stiffness of the surrounding soil medium and (b) provide sound bases for interpreting existing criteria and for developing nonlinear  $p$ - $y$  relations.

The major objectives of this paper are to (a) expand the concepts introduced by Kagawa and Kraft (10), (b) develop a new and improved procedure for determining such lateral soil springs, and (c) demonstrate the performance of such lateral soil springs. It is hoped that the results of this paper will provide a rational guideline for the estimation of the lateral soil springs to be used with the beam-on-Winkler foundation model for soil-pile interaction analyses.

## SOIL REACTION TO LATERALLY LOADED PILES

### Soil-Reaction Coefficient

Figure 1 shows how a pile responds to a horizontal force applied at its pile head for a pile in a linearly elastic, homogeneous medium. Figure 1 includes pile deflections normalized by corresponding ground-level deflections and the soil-reaction coefficient  $\delta$  defined by

$$p = E_s \delta y \quad (1)$$

where

- $p$  = the soil reaction to a unit length of a pile,
- $E_s$  = the Young's modulus of soil, and
- $y$  = pile deflection.

The soil-reaction coefficient  $\delta$  is a continuous function of depth, and  $\delta$  represents the interaction between the pile and the continuum soil medium. In addition,  $\delta$  is indicative of the soil stress that is normal to the pile.

Figure 1 shows that the soil-reaction coefficient starts with a positive value near the ground surface. The  $\delta$  value decreases with depth, and it may become negative at depth.

Negative  $\delta$  values occur where tensile normal stresses act in the soil adjacent to the pile.

As shown in Figure 1 for flexible piles, pile deflections vanish rapidly with depth, and the soil reaction to a pile is concentrated at shallow depths. Therefore, the soil at shallow depths participates in soil reaction more effectively than deeper soil. This results in larger  $\delta$  values at shallower depths for flexible piles. For rigid piles, soil reaction is mobilized more uniformly along the pile shaft, and smaller and more uniform soil-reaction coefficients result. Therefore, the relative deformability of the soil and the pile has a significant impact on  $\delta$ .

The pile responses in Figure 1 emphasize that a rational evaluation of the lateral soil springs must take full account of soil-pile interaction effects.

### Average Soil-Reaction Coefficient

Figure 1 has demonstrated that the soil stiffness against pile deflection is difficult to determine solely from the stiffness properties of soil without considering the soil-pile interaction effects determined by the geometry and the deformation properties of the pile. In addition, the soil-reaction coefficient, which represents the apparent lateral soil stiffness of the pile, varies dramatically with depth.

Figure 1 also suggests that we must exactly follow complex variations of  $\delta$  with depth when we are to correctly reproduce pile responses using the beam-on-Winkler foundation model. However, the use of a soil-reaction coefficient that is constant with depth would simplify the analysis procedure. Therefore, a soil-reaction coefficient that is constant with depth is introduced in the following. Such a constant profile represents an average behavior of the variation of  $\delta$  with depth.

To find such an average value  $\bar{\delta}$ , Kagawa and Kraft (10) and Kagawa (11) considered the pile responses in two separate systems, continuum and beam-on-Winkler foundation models. The soil reaction in the continuum (or exact) system is denoted by  $p$  and that of the beam-on-Winkler foundation is denoted by  $p'$ . The corresponding pile deflections in these two systems are represented by  $y$  and  $y'$ .

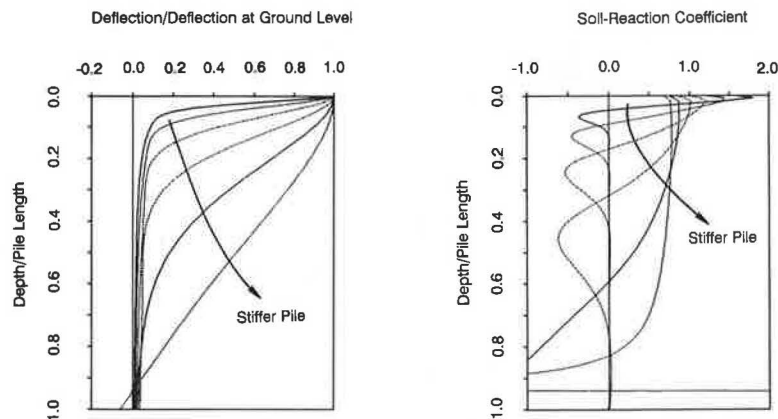


FIGURE 1 Pile deflection and soil-reaction coefficient.

The simplest way of deriving an average would be to assume that the sum of the soil reaction along the pile shaft is identical in the two systems. This condition may be represented by

$$\int_0^H (p - p') dx = 0 \quad (2)$$

in which  $H$  = pile length and  $x$  = depth. This condition also implies that the resultant lateral soil reaction along the pile in the beam-on-Winkler foundation model equals the pile-head shear. Assuming that the two systems produce the same pile deflections, we can derive the following average:

$$\bar{\delta} = \frac{\int_0^H p dx}{\int_0^H E_s y dx} \quad (3)$$

The next simplest average was derived by equating the work done by the soil reactions in the two systems. The work done by the soil reaction and the pile displacements in these systems under the same external loads may be equated as follows:

$$\int_0^H (py - p'y') dx = 0 \quad (4)$$

This condition is equivalent to the condition that the work done by the soil reaction in the beam-on-Winkler foundation method equals the work done by the pile-head shear. The average can then be obtained as

$$\bar{\delta} = \frac{\int_0^H py dx}{\int_0^H E_s y^2 dx} \quad (5)$$

In contrast to the average in Equation 3, the average in Equation 5 has the pile deflection as a weighting function; therefore, the soil-reaction coefficients at larger pile deflections have greater influence on the average.

### Improved Average Soil-Reaction Coefficients

The average in Equation 5 was developed originally for offshore piles that are usually long and flexible. The average has been found adequate to reproduce reliable pile responses in many cases (10,11). The use of  $\bar{\delta}$  in Equation 5 with the beam-on-Winkler foundation method, however, will not yield pile responses identical to the corresponding continuum model. The difference in pile responses from these two systems tends to be large for very long and flexible piles. Therefore, the goal of this paper is to obtain the average soil-reaction coefficient  $\bar{\delta}$  that yields improved pile responses for a wide range of soil-pile parameters.

The objective of establishing such an average may be mathematically equivalent to minimizing the following weighted error integral:

$$E = \int_0^H W(x)(p - p')^2 dx \quad (6)$$

where  $p'$  is the soil reaction in the beam-on-Winkler foundation model,  $E_s \bar{\delta} y'$ . Assuming that  $y'$  equals  $y$ , we can minimize this error integral by determining  $\bar{\delta}$  from the following condition:

$$\frac{\partial E}{\partial \bar{\delta}} = 0 \quad (7)$$

Equation 7 gives the following average:

$$\bar{\delta} = \frac{\int_0^H W(x)py dx}{\int_0^H W(x) E_s y^2 dx} \quad (8)$$

The average in Equation 8 gives the average in Equation 5 when the weighting function  $W(x)$  equals unity. Therefore, the work consideration used in the derivation of the average in Equation 5 was a special case of minimization of the error integral in Equation 6. The true virtue of Equation 8, however, gives us a unified approach to obtaining average  $\bar{\delta}$ . Equation 8 allows us to devise various averages that satisfy specific purposes.

## PERFORMANCE EVALUATION OF AVERAGE SOIL-REACTION COEFFICIENTS

### Numerical Procedures

Pile responses have been computed by the computer program PILE, coded specifically for this study, and the performance of several average  $\bar{\delta}$ 's has been studied to find the best soil-reaction model for the beam-on-Winkler foundation analysis of laterally loaded piles. The program is based on linearly elastic models of soil medium and a pile. A pile was divided into a sufficient number of elements to achieve satisfactory accuracy of computed pile responses. The number of elements used in this study ranged from 70 to 135, depending on pile length. The soil reaction to the pile was evaluated by first constructing the flexibility matrix of the soil medium and then by inverting the matrix to obtain the stiffness matrix for soil reaction. The flexibility coefficients were computed by integrating, over the surface of an incremental length of a pile, Mindlin's solution to a homogeneous, elastic half-space (12). The pile was modeled by the standard, finite-element, beam elements.

The following four different averages of the soil-reaction coefficients were computed for a continuum soil condition:

- $\bar{\delta}$  in Equation 3 (Case 1),
- $\bar{\delta}$  in Equation 5 (Case 2),
- $\bar{\delta}$  in Equation 8 with  $W(x) = y$  (Case 3), and
- $\bar{\delta}$  in Equation 8 with  $W(x) = p$  (Case 4).

Computed pile responses were then compared with those from the beam-on-Winkler foundation model with corresponding average  $\bar{\delta}$ .

Case 1 is the simplest average of all. Case 2 assumes unity for the weighting function in Equation 8. Case 3 uses the pile

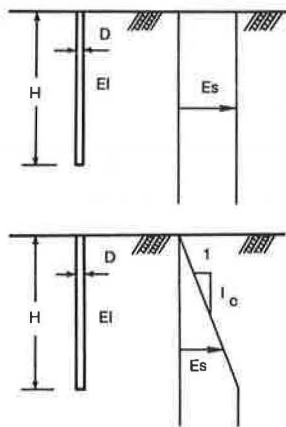
deflection  $y$  as the weighting function in the error integral in Equation 8, and Case 4 uses the soil reaction  $p$  as the weighting function.

### Key Soil-Pile Parameters

The soil-pile conditions used in this study are schematically shown in Figure 2. These involve the cases with soil modulus constant with depth (homogeneous modulus cases) and those with soil modulus linearly increasing with depth (linearly increasing modulus cases). The homogeneous modulus cases may apply to overconsolidated soil conditions in which the soil stiffness does not appreciably change with depth. On the other hand, the linearly increasing modulus cases may be valid for normally consolidated clay and sand sites in which the soil stiffness increases nearly proportionally with depth. The physical properties of such a soil medium are represented by the shear modulus (or Young's modulus)  $G_s$  (or  $E_s$ ) and Poisson's ratio  $\nu$  for the homogeneous modulus cases and by the rate of increase in Young's modulus with depth  $I_c$  and Poisson's ratio  $\nu$  for the linearly increasing modulus cases. The pile is characterized by the width  $D$ , the length  $H$ , and the flexural rigidity  $EI$ . A brief dimension analysis reveals that pile responses are controlled by the aspect ratio of the pile  $H/D$ , Poisson's ratio of soil, and the degree of rotational constraint at the pile head (fixed-head or free-head condition). In addition, the relative deformability of soil and the pile is related to the soil-pile flexibility coefficient defined by

$$K_r = \frac{EI}{E_s H^4} \quad \bar{K}_r = \frac{EI}{E_s D^4} \quad \tilde{K}_r = \frac{EI}{I_c D^5} \quad (9)$$

The soil-pile flexibility coefficients  $K_r$  and  $\bar{K}_r$  are useful for the homogeneous modulus cases. The soil-pile coefficient  $\bar{K}_r$  will be called "local" soil-pile flexibility because the coefficient involves only the soil-pile conditions at a depth.  $\tilde{K}_r$  will also be called a local soil-pile flexibility coefficient, and it will be used for the linearly increasing modulus cases. Smaller



(b) Linearly Increasing Modulus Cases

**FIGURE 2** Soil-pile conditions: *top*, homogeneous modulus cases; *bottom*, linearly increasing modulus cases.

**TABLE 1** RANGES OF KEY PARAMETER VALUES

Key Parameters	Parameter Values
H/D	25, 50, 100 & 200
$K_r$	10e-7 to 10e-2
$\bar{K}_r$ & $\tilde{K}_r$	10e+1 to 10e+6
Pile-Head Cond.	Free & Fixed Head
Poisson's Ratio of Soil	0.3, 0.4 & 0.5

soil-pile flexibility coefficients correspond to more flexible pile (or stiffer soil) conditions.

The ranges of values of the dimensionless parameters used in this study are summarized in Table 1. These ranges are expected to cover sufficient variations of soil-pile conditions in practice.

### Homogeneous Soil Stiffness Cases

The average soil-reaction coefficients (Cases 1 through 4) have been computed for a variety of soil-pile conditions. Figure 3 shows typical results of such analyses.  $\bar{\delta}$  values for Cases 1 through 4 are shown for an aspect ratio of 100, a Poisson's ratio of 0.5, and the free-head condition.  $\bar{\delta}$  values from Case 1 are nearly constant even if the soil-pile flexibility coefficient changes from  $10^{-7}$  to  $10^{-2}$ . This indicates that Case 1 does not reflect the soil-pile interaction effects due to the relative deformability of soil and the pile. On the other hand, Cases 2 through 4 yielded  $\bar{\delta}$  values that dramatically decrease as the pile stiffness (or the soil-pile flexibility coefficient) increases. This analysis indicated that the Poisson's ratio has a negligible influence on  $\bar{\delta}$  values and that the fixed-head condition results in smaller  $\bar{\delta}$  values.

Figure 4 compares the lateral pile-head stiffness obtained from the continuum soil cases and from the beam-on-Winkler foundation models with  $\bar{\delta}$  from Cases 1 through 4. The figure includes results for the free-head and fixed-head conditions and for aspect ratios of 25 and 100. Figure 4 shows that Case 1 significantly underestimates the lateral pile-head stiffness. A similar conclusion applies to Case 2 for short and flexible piles. On the other hand, Case 4 tends to overestimate the lateral pile-head stiffness for all cases. This tendency is pro-

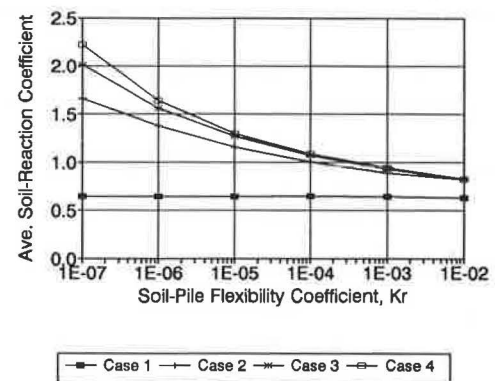


**FIGURE 3** Average soil-reaction coefficients for  $H/D = 100$  and free-head conditions (homogeneous  $E_s$ ).

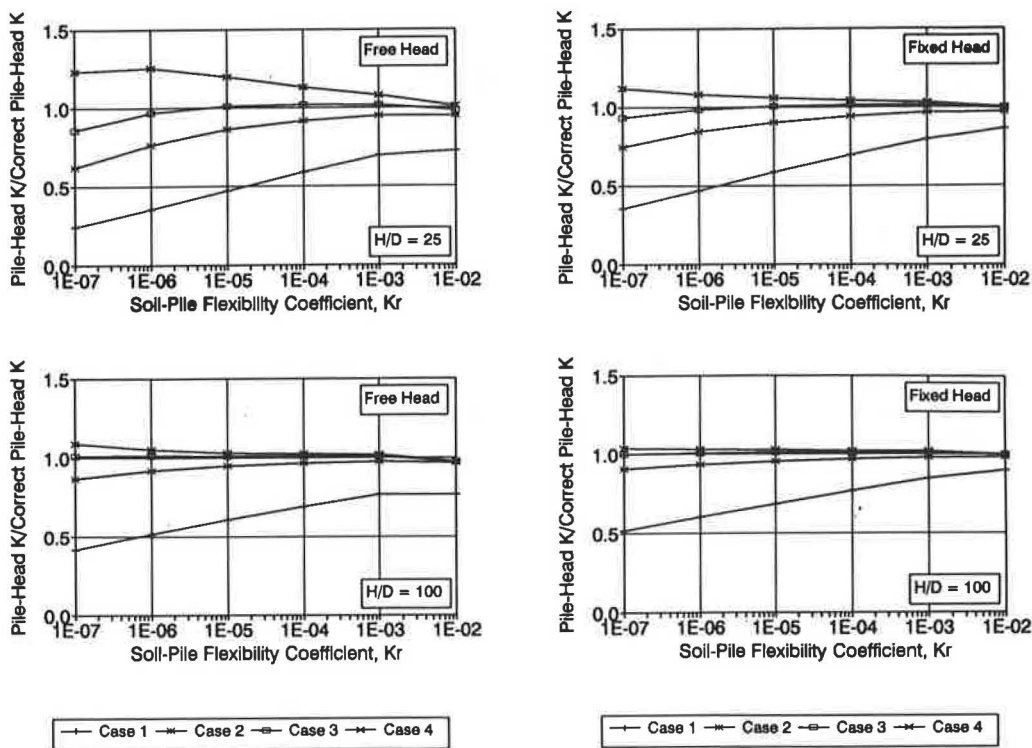


FIGURE 4 Comparisons of pile-head stiffnesses from continuous and beam-on-Winkler foundation models (homogeneous  $E_s$ ).

nounced for short and flexible piles. Case 3, however, gives excellent predictions of lateral pile-head stiffness.

Similar comparisons are made in Figure 5 for the maximum bending moments in the pile computed by the continuum soil cases and by the beam-on-Winkler foundation models with  $\bar{\delta}$  from Cases 1 through 4. In all cases the maximum moment in the pile is overestimated by the beam-on-Winkler foundation models. Case 1 yielded significant overestimation for short and flexible piles with the free-head condition. Cases 2 through 4 provide much better agreements than Case 1, but we cannot neglect this overestimation for short and flexible piles. Case 4 resulted in the best agreement, but the difference in performance between Cases 3 and 4 is very small. Most piles in practice have a soil-pile flexibility coefficient on the order of  $10^{-6}$  to  $10^{-3}$ . For this range of  $K_r$ , overestimation is on the order of less than 20 percent.

The comparisons in Figures 4 and 5 indicated that Case 3 gives the best predictions of pile responses for a wide range of soil-pile parameter values. Therefore, the average  $\bar{\delta}$  from Case 3 is summarized in Figure 6 for the free-head and fixed-head conditions. Figure 6 includes results for aspect ratios of 25, 50, 100, and 200. The  $\bar{\delta}$  values for these aspect ratios are nearly identical except for very rigid piles. This identity resulted from plotting  $\bar{\delta}$  against the local soil-pile flexibility coefficient  $\bar{K}_r$ .

Natural soil conditions do not involve homogeneous soil stiffness with depth. Therefore, a guideline may be needed for the selection of an appropriate soil modulus for  $\bar{K}_r$  when  $\bar{\delta}$  in Figure 6 is to be used in design. Such a guideline may be derived by looking at the variation of the numerator of

Equation 8 with depth. This quantity starts with zero at the ground surface and increases with depth. At some depth this quantity reaches its maximum value, and its value will not change after that. The portion of the soil before this quantity reaches the maximum may be considered to actively resist pile deflection. Therefore, the stiffness of this portion of soil can be used in  $\bar{K}_r$ . The depth at which the numerator of Equation 8 reaches the maximum will be called the effective pile length for the purpose of estimating  $\bar{K}_r$ . The effective pile lengths thus computed are summarized in Figure 7 for a range of soil-pile conditions. Unless a pile is very rigid (i.e.,  $\bar{K}_r$  exceeds about  $10^{-4}$ ), the effective pile length is typically less than 20-pile-diameter depth.

#### Linearly Increasing Soil Stiffness Cases

A series of parametric studies have also been made for the linearly increasing soil modulus cases. Their results are summarized below.

Figure 8 shows comparisons of the pile-head stiffness computed by the continuum and the beam-on-Winkler foundation models with  $\bar{\delta}$  from Cases 1 through 4. As we observed in the homogeneous modulus cases, Case 1 does not provide reliable estimates of pile-head stiffness for all the conditions used in this study. Case 2 yielded best agreements, and Cases 3 and 4 slightly overestimate the pile-head stiffness. The degree of overestimation is on the order of 5 percent.

Figure 9 shows similar comparisons for the maximum pile moments obtained from the continuum and the beam-on-



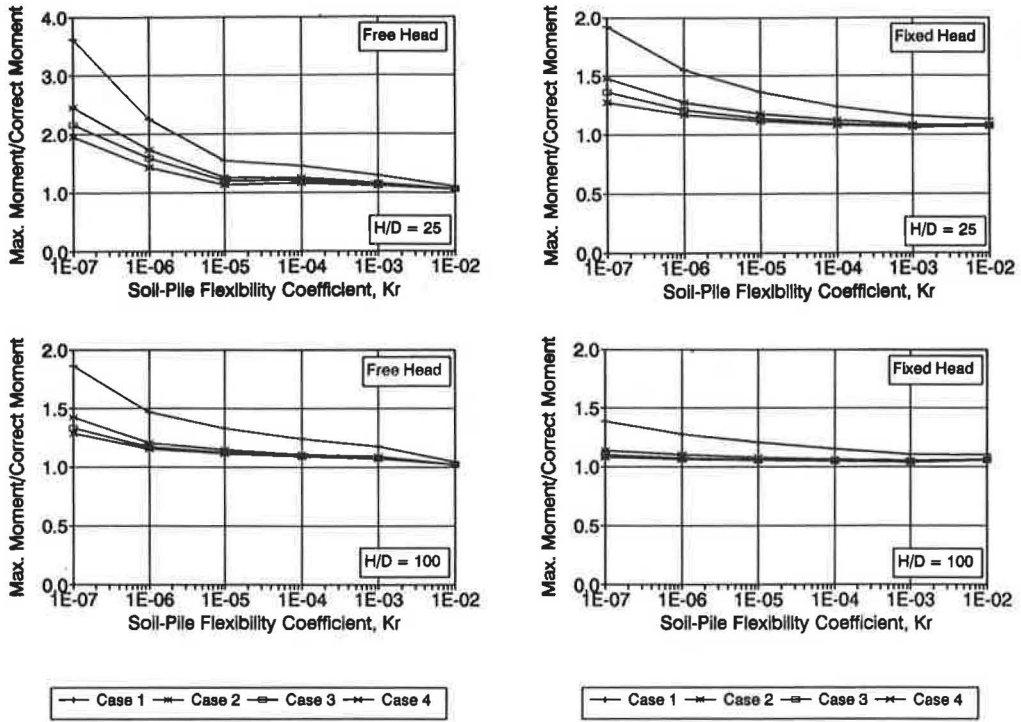


FIGURE 5 Comparisons of pile moment from continuous and beam-on-Winkler foundation models (homogeneous  $E_s$ ).

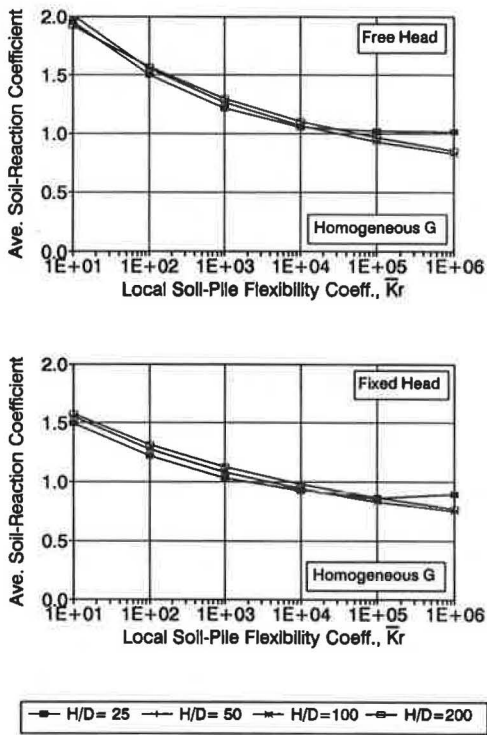


FIGURE 6 Summary of average soil-reaction coefficients (homogeneous  $E_s$ ).

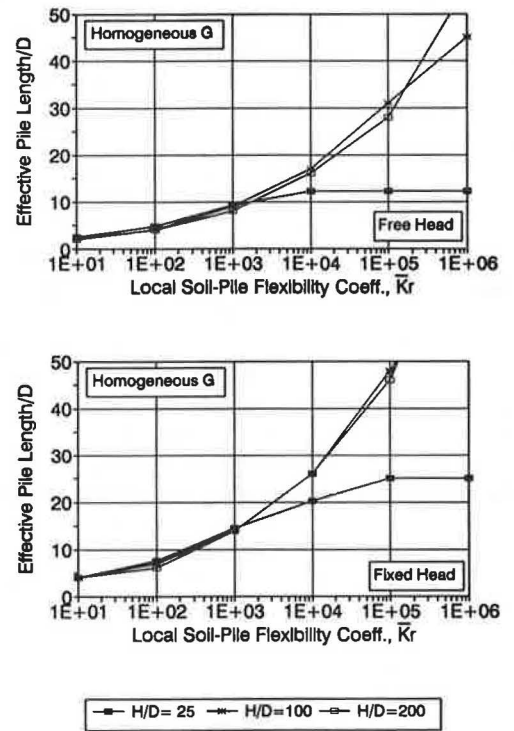


FIGURE 7 Effective pile length (homogeneous  $E_s$ ).

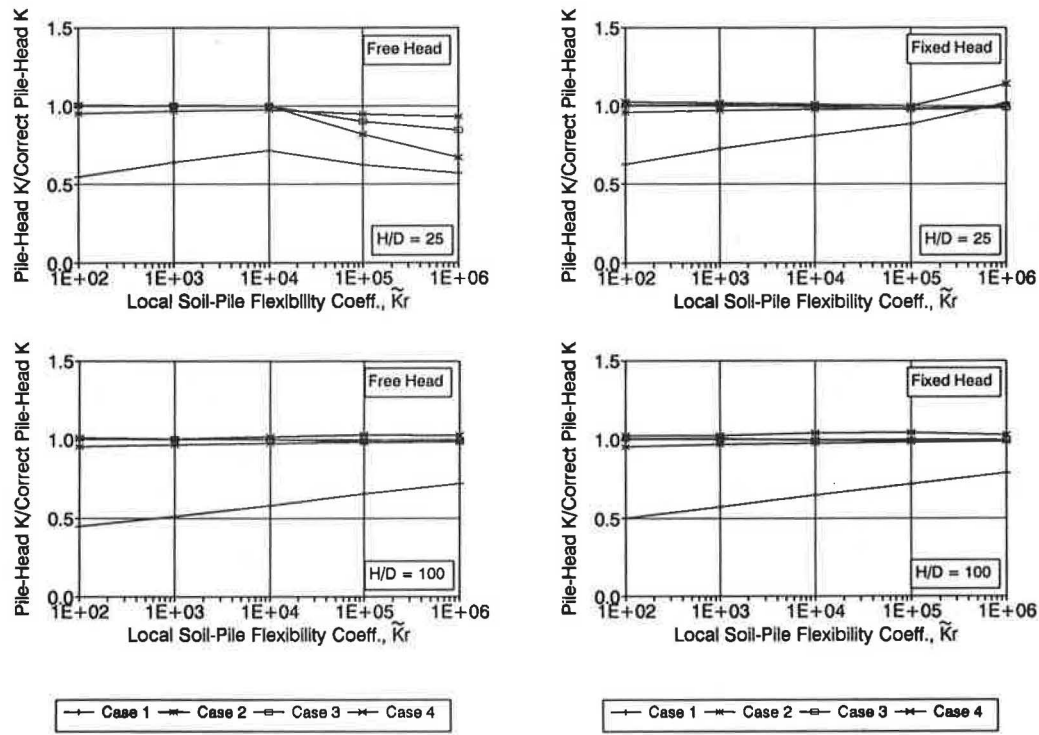


FIGURE 8 Comparisons of pile-head stiffnesses from continuous and beam-on-Winkler foundation models (linearly increasing  $E_s$ ).

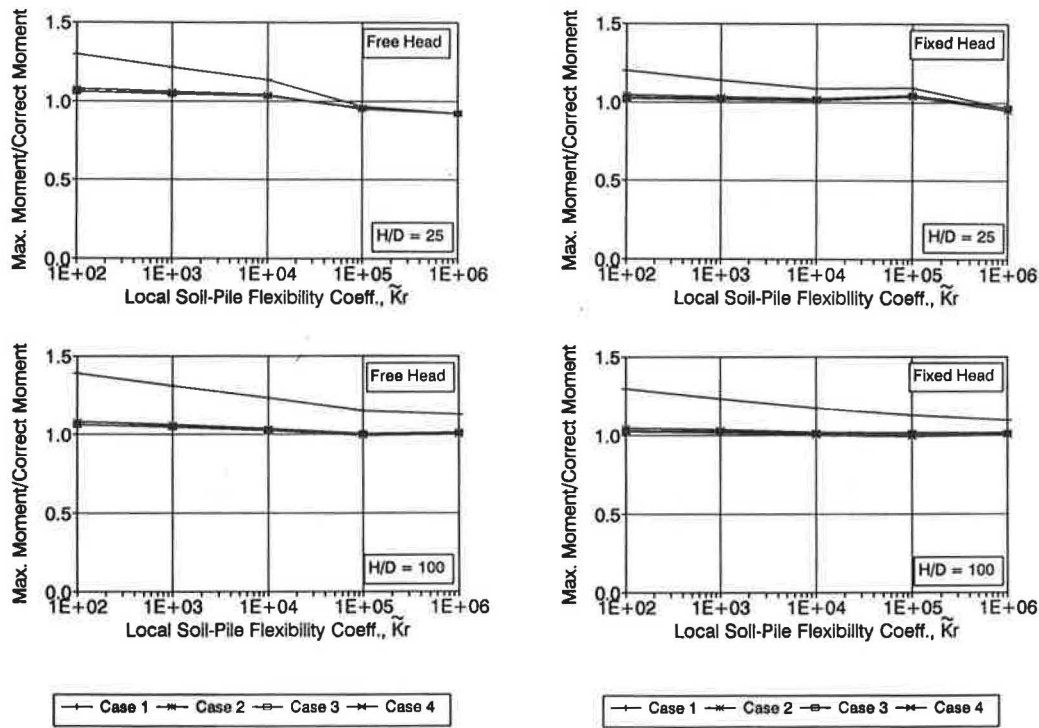


FIGURE 9 Comparisons of pile moment from continuous and beam-on-Winkler foundation models (linearly increasing  $E_s$ ).

Winkler foundation models. Cases 1 through 4 overestimate the maximum moment in the pile except for very rigid pile (or soft soil) conditions. The degree of overestimation in this case is much less than that in the homogeneous modulus cases (see Figure 5). Cases 2 through 4 estimate almost perfectly the maximum moment in the pile.

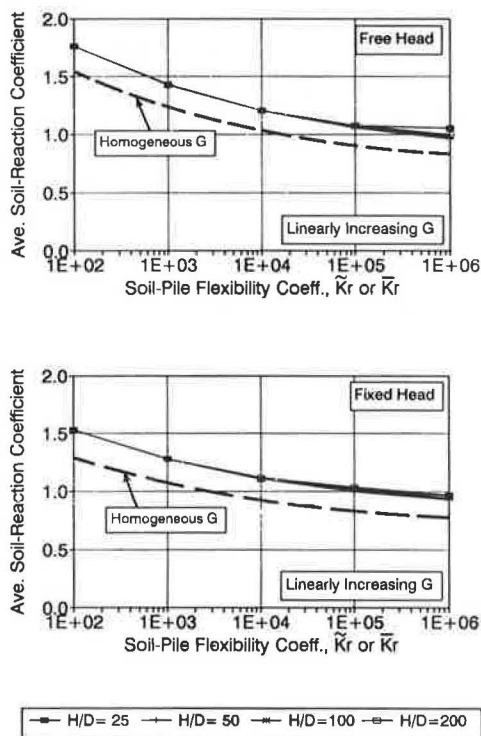
Although Case 2 resulted in excellent predictions of pile-head stiffness and pile moments, the overall performance of Case 3 for both the homogeneous and linearly increasing modulus cases is considered to be the best. The average  $\bar{\delta}$  from Case 3 is plotted against  $\bar{K}_r$  in Figure 10. The figure also includes  $\bar{\delta}$  in Figure 7 for comparison. The  $\bar{\delta}$ 's for the homogeneous cases are less than those for the linearly increasing modulus cases by about 0.2 for both the free-head and fixed-head conditions.

Figure 11 summarizes the effective pile lengths for the linearly increasing modulus cases. The effective pile length is typically less than 15-pile-diameter depth unless the pile is very rigid (i.e.,  $\bar{K}_r$  exceeds about  $10^4$ ).

**APPLICATIONS**

Results of this study can be readily used in the design analysis of laterally loaded piles. The average  $\bar{\delta}$  in Figures 6 and 10 can be used to determine the lateral soil springs for the beam-on-Winkler foundation model of a soil-pile system. For a given set of soil stiffness data, the lateral soil springs can be determined from

$$K = \frac{P}{y} \Delta H = E_s \bar{\delta} \Delta H \tag{10}$$



**FIGURE 10** Summary of average soil-reaction coefficient (linearly increasing  $E_s$ ).

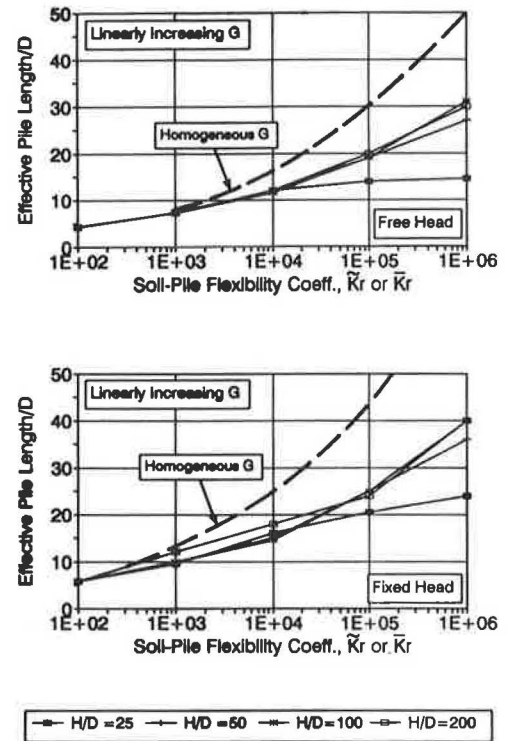


**FIGURE 11** Effective pile length (linearly increasing  $E_s$ ).

where the lateral soil spring  $K$  is defined over the incremental pile length  $\Delta H$ . Evaluation of  $E_s$  (Young's modulus of soil) invites discussion, but  $E_s$  should be based on a rational estimate of the magnitude of the soil strains involved in the problem under investigation. A typical guideline to serve this purpose is given by (5,10)

$$\gamma = (1 + \nu)y/(\alpha D) \tag{11}$$

where

- $\gamma$  = the representative soil shear strain around the pile,
- $\nu$  = Poisson's ratio of soil, and
- $\alpha$  = an empirical factor that typically ranges from 2.0 to, say, 6.0.

The lateral soil springs thus determined can then be used as input to readily available beam-column computer programs.

**CONCLUSIONS**

A numerical study was made for linearly elastic soil-pile conditions to clarify the lateral soil-reaction behavior of a pile.

The study indicated that the apparent lateral stiffness of soil, represented by the soil-reaction coefficient  $\delta$ , is strongly influenced not only by the soil stiffness but also the geometry and the stiffness of the pile. In addition,  $\delta$  varies significantly with depth.

The paper presented a new approach for obtaining average soil-reaction coefficients, which are constant with depth even for layered soil conditions, that can be used with the beam-on-Winkler foundation model of a soil-pile system. With this



average soil-reaction coefficient, the beam-on-Winkler foundation model will reproduce with excellent accuracy the pile responses computed from the corresponding continuum system. Therefore, the results of this study can be instantly used by practicing engineers.

Although this study is limited to linearly elastic soil-pile conditions, the results can be expanded to nonlinear soil conditions, as suggested by Kagawa and Kraft (10,13).

## REFERENCES

1. K. Terzaghi. Evaluation of Coefficients of Subgrade Reaction. *Geotechnique*, Vol. 5, 1955.
2. B. B. Broms. Lateral Resistance of Piles in Cohesive Soils. *Journal, Soil Mechanics and Foundations Division*, ASCE, Vol. 90, No. SM2, 1964, pp. 27-63.
3. B. B. Broms. Lateral Resistance of Piles in Cohesionless Soils. *Journal, Soil Mechanics and Foundations Division*, ASCE, Vol. 90, No. SM3, 1964, pp. 123-156.
4. B. McClelland and J. A. Focht, Jr. Soil Modulus for Laterally Loaded Piles. *Transactions*, ASCE, Vol. 123, 1958.
5. H. Matlock. Correlations for Design of Laterally Loaded Piles in Soft Clay. *Proc., 2nd Offshore Technology Conference*, Houston, Tex., 1970, pp. 577-594.
6. L. C. Reese, W. R. Cox, and F. D. Koop. Analysis of Laterally Loaded Piles in Sand. *Proc., 6th Offshore Technology Conference*, Houston, Tex., 1974, pp. 473-483.
7. D. A. Brown, C. Morrison, and L. C. Reese. Lateral Load Behavior of Pile Group in Sand. *Journal, Geotechnical Engineering Division*, ASCE, Vol. 114, No. 11, 1988, pp. 1261-1276.
8. C.-F. Tsai, R. F. Scott, D. Steussy, and J. M. Ting. *Full-Scale Pile Vibration Tests*. Earth Technology Corp. and California Institute of Technology, Long Beach and Pasadena, Calif., 1981.
9. *API Recommended Practice for Planning, Designing and Constructing Fixed Offshore Platform* (16th ed.). American Petroleum Institute, Washington, D.C., 1986.
10. T. Kagawa and L. M. Kraft, Jr. Lateral Load-Deflection Relationships of Piles Subjected to Dynamic Loadings. *Soils and Foundations*, Vol. 20, No. 4, 1980, pp. 19-36.
11. T. Kagawa. Dynamic Soil Reaction to Axially Loaded Piles. *Journal, Geotechnical Engineering Division*, ASCE, Vol. 117, No. 7, 1991, pp. 1001-1020.
12. R. D. Mindlin. Force at a Point in the Interior of a Semi-Infinite Solid. *Physics*, Vol. 7, 1936.
13. T. Kagawa and L. M. Kraft, Jr. Lateral Pile Response During Earthquakes. *Journal, Geotechnical Engineering Division*, ASCE, Vol. 107, No. GT12, 1981, pp. 1713-1731.

---

*Publication of this paper sponsored by Committee on Foundations of Bridges and Other Structures.*